Materials and Structures (2016) 49:2637–2651
DOI 10.1617/s11527-015-0673-8

ORIGINAL ARTICLE

Ag/AgCl ion-selective electrodes in neutral and alkaline environments containing interfering ions

Yurena Seguí Femenias · Ueli Angst · Francesco Caruso · Bernhard Elsener

Received: 13 April 2015 / Accepted: 4 July 2015 / Published online: 10 July 2015

Abstract Chloride ingress can lead to serious degradation of various materials and structures. Continuous measurements of local chloride concentrations is thus of uttermost importance for laboratory research, monitoring of structures, and predictions of the residual life span for the most common building materials. This work investigates the applicability of Ag/AgCl ion-selective electrodes for the non-destructive continuous measurement of local chloride concentrations in concrete and stone when exposed to chloride-bearing environments such as seawater. The work studies the stability of Ag/AgCl ion-selective electrodes in neutral and alkaline solutions and the sensitivity to the main interfering ions coming from the environment and from the material itself. The results indicate negligible interference from fluoride, sulfate, and hydroxyl but considerable from bromide and sulfide. In chloride-free alkaline solutions, Ag/AgCl ion-selective electrodes are not stable over time, but—upon chloride arrival—they permit again reliable measurements of the chloride concentration. The results concerning interference are discussed by taking into account typical exposure environments and it is concluded that the ion-selective electrodes can satisfactorily be used to monitor chloride concentrations in built structures made out of concrete or stone.

Keywords Chloride monitoring · Ion-selective electrode · Interfering species · Sensitivity · Long-term stability · Selectivity coefficient

Y. Seguí Femenias (✉) · U. Angst · F. Caruso · B. Elsener
ETH Zürich, Institute for Building Materials (IfB), Stefano-Franscini-Platz 3, 8093 Zurich, Switzerland
e-mail: syurena@ethz.ch

U. Angst
Swiss Society for Corrosion Protection (SGK), Technoparkstrasse 1, 8005 Zurich, Switzerland

B. Elsener
Department of Chemical and Geological Sciences, University of Cagliari, 09100 Monserrato, CA, Italy

1 Introduction

Chloride ingress can lead to deterioration of various materials and structures. In non-carbonated reinforced concrete, when the chloride concentration reaches the so-called critical chloride content at the steel surface, depassivation of the steel occurs and chloride-induced corrosion initiates [1]. Natural stone can also be damaged by chloride ingress. When local chloride content reaches a certain level, supersaturation and crystallization of various salts can occur. Salt crystallization in the stone porosity may then exert substantial expansive stresses and seriously deteriorate the stone microstructure [2–5]. For similar reasons, structural degradation can also result from chloride ingress in masonry [6, 7]. In addition, when combined with other external constraints such as, for instance, freeze–thaw cycles, it is known that the presence of

chlorides can enhance the resulting damage in both stone and concrete [4, 8, 9].

In this context, the measurement of local chloride concentrations appears essential in building materials and structures. This is further enhanced by the latest advances and research in science, engineering, and technology. From a scientific point of view, the concept of the critical chloride content in concrete is at the origin of large debates [10–12]. Non-destructive and local measurements of chloride concentrations at the surface of the embedded reinforcement steel play an important role in research on this matter. From an engineering point of view, service life prediction models are increasingly used, in the design or in the infrastructure management stage. These models are based on predicting chloride ingress into concrete [13–15]. Therefore, continuous measurements of local chloride concentrations in laboratory specimens or in field structures are needed for their validation. Furthermore, the ever-increasing awareness for environmental concerns and sustainability resulted in a growing market share of blended cements [16, 17], which raised new questions on durability and mass transfer properties of these non-traditional materials [18, 19]. These questions cannot be answered using the existing one-century experience from Portland cement. However, they need to be quickly solved to bring these new binders from laboratory research to practice and improve the environmental performance of concrete [17].

The current methods for determining the local chloride contents in concrete and stone traditionally require destructive sampling (drilling, grinding, etc.) and do not allow obtaining continuous information at an identical location over time [4, 20, 21]. Non-destructive techniques for chloride detection are therefore being developed [22–28]. Some of the proposed techniques are able to measure relative variations in local chloride contents rather than the absolute local chloride contents [26, 28]. In this regard, it is considered that the use of Ag/AgCl ion-selective electrodes (ISEs) may be a promising solution [29–33]. Potentiometric measurement of chloride with ISEs is a well-established method that has mostly been limited to laboratory conditions. However, some attempts of in situ use of Ag/AgCl ISE have been recently made for the specific case of concrete [22–25, 27]. Nevertheless, surfaces of ISEs are notably sensitive to chemical species other than chloride [27, 34–37]. The applicability of Ag/AgCl ISE in complex chemical environments can thus be impaired by the presence of interfering species, coming either from the considered structure environment or from the material itself (for instance, hydroxyl interference in concrete). This paper investigates the applicability of the Ag/AgCl ISE for monitoring chloride concentrations in built structures made out of concrete or stone and exposed to chloride-bearing environments such as seawater. Therefore, it studies the long-term stability of Ag/AgCl ISE at high pH values and the possible interference arising from the presence of bromide, sulfate, sulfide, fluoride, and hydroxyl. From the obtained results, the ability of Ag/AgCl ISE to monitor the local chloride content in the pore solutions of concrete and stone is here discussed.

2 Theoretical background

2.1 The silver/silver chloride ion-selective electrode

The Ag/AgCl ISE used in this work belongs to the category of ion-selective electrodes with solid ion exchangers [29–31]. The Ag/AgCl ISE used here consists of silver covered by a layer of silver chloride. Since the AgCl coating has a low solubility, the electrolyte around the ISE is easily saturated with it and the potential E of the ISE is given by the Nernst equation:

$$E = E^0_{\mathrm{Ag/AgCl}} - \frac{RT}{F}\ln a_{\mathrm{Cl^-}} \quad (1)$$

where R is the gas constant, F the Faraday constant, T the absolute temperature, $a_{\mathrm{Cl^-}}$ the activity of the chloride, and $E^0_{\mathrm{Ag/AgCl}}$ expresses the standard potential of the Ag/AgCl electrode. $E^0_{\mathrm{Ag/AgCl}}$ is defined by the following equation [38]:

$$E^0_{\mathrm{Ag/AgCl}} = E^0_{\mathrm{Ag/Ag^+}} + \frac{RT}{F}\ln K_{S\_\mathrm{AgCl}} \quad (2)$$

where $E^0_{\mathrm{Ag/Ag^+}}$ is the standard potential of the $\mathrm{Ag/Ag^+}$ electrode and K_{S_AgCl} is the solubility product of AgCl.

The Ag/AgCl ISE responds to the primary ion (chloride ion) with a Nernstian behavior only above a

minimum concentration of it, the detection limit [31, 32, 39, 40]. Furthermore, the ISE is also sensitive to other species that can form precipitates of lower solubility with the constituent ionic species [27, 34–37]. This interference is traditionally considered with the selectivity coefficient, $K^{pot}_{Cl^-,Y}$ (with Y standing for the interfering species), included in the Nikolsky–Eisenman equation [31, 32, 41]:

$$E = E^0_{Ag/AgCl} - \frac{RT}{F}\ln\left(a_{Cl^-} + \sum\left(K^{pot}_{Cl^-,Y} \times a_Y^{-1/z_Y}\right)\right) \quad (3)$$

where a_Y is the activity of the interfering ionic species and z_Y its charge.

2.2 Influencing parameters

The ISE potential E depends on the chloride activity, the temperature, and the sensitivity to other species [Eq. (3)].

2.2.1 Chloride activity

In concentrated solutions, the high ionic strength causes large differences between activity and concentration. This phenomenon is taken into account by the use of the ionic activity a_X, which is related to the concentration c_X of a species X by the activity coefficient γ_X [38]:

$$a_X = \gamma_X \cdot {c_x}/{c^0} \quad (4)$$

where c^0 is the standard state composition (chosen as 1 mol L^{-1}).

2.2.2 Interfering species

Many silver salts have very low solubilities [38]; therefore, in their presence, the ISE is likely to be affected. The AgCl membrane responds mainly to Cl^-, Br^-, I^-, OH^-, and S^{2-} [27, 32, 35, 40, 41]. According to Eq. (3), the potential of the ISE will exhibit a Nernstian behavior when the following relation is satisfied [27]:

$$a_{Cl^-} \gg \sum\left(K^{pot}_{Cl^-,Y} \times a_Y^{-1/z_Y}\right) \quad (5)$$

2.2.3 Temperature

Both the Ag/AgCl electrode standard potential $E^0_{Ag/AgCl}$ and the *RT/F* term in Eq. (1) depend on temperature. Concerning $E^0_{Ag/AgCl}$, the effect of temperature has been addressed in detail in other studies and data is available to make the appropriate corrections; temperature coefficients between −0.6 and −0.65 mV $°C^{-1}$ have been reported [27, 42]. As an example, a decrease in temperature by 10 °C would thus lead to a decrease of ca. 6 mV in $E^0_{Ag/AgCl}$ and of ca. 3 mV in the *RT/F* term. Nevertheless, these errors can be corrected by always taking into account the temperature when applying the sensors under temperature fluctuating conditions. Furthermore, temperature effects can be reduced by using silver/silver chloride based reference electrodes (e.g. Ag/AgCl/sat. KCl) since in this case, the reference electrode and the ISE have the same standard potential, $E^0_{Ag/AgCl}$ and thus temperature only affects the *RT/F* term in Eq. (1).

Finally, it should be noticed that when a potentiometric measurement is performed the potentials of both the chloride ISE and the reference electrode against which the measurement is performed, depend on temperature [27]. When a temperature difference between the ISE and the reference electrode exists, errors in the measurement arise. Atkins et al. [35] showed that small temperature differences can lead to significant errors. Therefore, it is recommended that ISE and reference electrode are placed as close as possible (see also Sect. 4.3.3).

3 Materials and protocols

3.1 Electrodes, instruments and materials

3.1.1 The Ag/AgCl ion-selective electrode (ISE)

The Ag/AgCl ISE used is a commercially available ISE (Metrohm AG, Zofingen, Switzerland) consisting of Ag wire coated with AgCl deposited by anodizing. The tip of the ISE was additionally dipped in a melt of AgCl in order to achieve a more stable membrane [24, 27]. A stereomicroscopy image of the Ag/AgCl electrode is shown in Fig. 1.

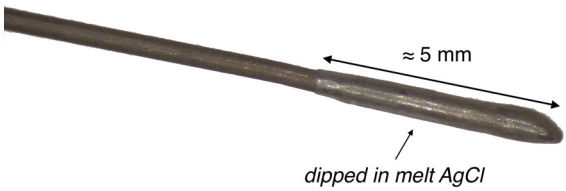

Fig. 1 Stereomicroscopy image of the Ag/AgCl ISE used in this work consisting of a Ag wire coated with AgCl

3.1.2 Instruments for the potentiometric measurements

The potential of the ISEs was measured against the silver/silver chloride/saturated potassium chloride (Ag/AgCl/sat. KCl) reference electrode (+0.197 V vs. SHE). A Luggin capillary (filled with the test solution) was used when the reference electrode was immersed in the test solution to avoid chloride contamination derived from the contact between test solution and KCl from the reference electrode.

It should be noted that, when the reference electrode is immersed in the test solution, liquid junction potential [40] establishes at the test solution/reference electrode interface and adds arithmetically to the measured potential. The situation is schematically depicted in Fig. 2.

The measurements were performed with a PGSTAT 30 Autolab potentiostat/galvanostat (Metrohm Autolab, Utrecht, the Netherlands) with high input impedance (>100 GΩ) connected to a Windows PC for data acquisition. The program for data acquisition was Autolab Nova v.1.10. All the experiments were carried out at room temperature (20–21 °C).

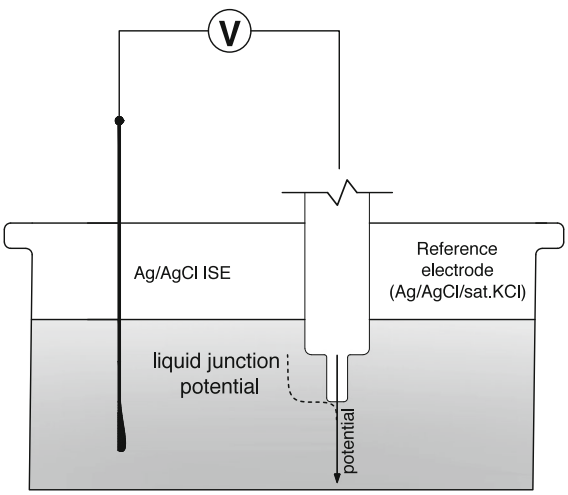

Fig. 2 Set-up for the potentiometric measurements with the schematic representation of the liquid junction potential established at the interface of the reference electrode and the solution

3.1.3 Materials

The sodium chloride (ACS, ISO Reag. Ph. Eur. grade) used for the preparation of the solutions was purchased from Merck (Merck KGaA, Darmstadt, Germany). The chemicals used for the preparation of interfering species solutions were: sodium hydroxide (≥99.0 %, Merck), potassium bromide (99.999 %, Fluka, Sigma-Aldrich Chemie GmbH, Buchs, Switzerland), potassium sulfate (≥99.0 %, Fluka), sodium fluoride (≥99.0 %, Sigma-Aldrich), and sodium sulfide nonahydrate (≥98.0 %, Sigma-Aldrich). All the solutions were prepared with de-ionized water (conductivity ≈ 2 μS/cm).

3.2 Methods

3.2.1 Calibration in solution

The Ag/AgCl ISEs were calibrated in neutral and alkaline solutions that contained known concentrations of sodium chloride ranging from 0.002 to 4 mol L^{-1}.

Liquid junction potentials E_{junction} [40] at the interface between the reference electrode and the calibration solution were calculated according to the Henderson equation [40]. For this calculation, it is considered that the concentration of KCl is 4.16 mol L^{-1} when saturated in water at room temperature (20 °C) [38].

The used solutions and the liquid junction potentials calculated are presented in Table 1.

The chloride activity was calculated according to Eq. (4). The activity coefficients of the chloride ion (γ_{Cl^-}) were interpolated from the data given by de Vera et al. [43]. For the alkaline solutions, the effect of the accompanying ions was neglected and activity coefficients were calculated considering the total hydroxyl concentration. The data is provided in Table 2.

The calibration curves were obtained by linear regression analysis:

$$E = E_{\text{measured}} - E_{\text{junction}} = m \cdot \log a_{Cl^-} + b \qquad (6)$$

Table 1 Calibration solutions and corresponding liquid junction potentials for the Ag/AgCl/sat. KCl

NaCl concentration (mol L^{-1})	NaOH concentration (mol L^{-1})	$E_{junction}$ at 20 °C (mV)
0.002	–	−3.7
0.01	–	−2.9
0.1	0.01	−1.2
0.1	0.1	0.7
0.1	1	8.4
0.5	–	0.1
0.5	0.01	0.3
0.5	0.1	1.5
0.5	1	8.4
1	–	1.2
1.5	–	1.9
4	–	4.2

Table 2 Activity coefficients of the chloride ion γ_{Cl^-} used in this work. Values of pH other than 7 were obtained by addition of sodium hydroxide. The values of γ_{Cl^-} are interpolated from the data given by de Vera et al. [43]

NaCl concentration (mol L^{-1})	pH	γ_{Cl^-}
0.002	7	0.958
0.01	7	0.901
0.1	7	0.767
0.5	7	0.648
1	7	0.603
1.5	7	0.587
2	7	0.572
4	7	0.576
5	7	0.591
0.1	≈12	0.740
0.1	≈13	0.727
0.1	≈14	0.603
0.5	≈12	0.642
0.5	≈13	0.637
0.5	≈14	0.585

3.2.2 *Sensitivity to interfering species*

The interference was investigated for hydroxyl, bromide, sulfate, fluoride, and sulfide. These were considered the main species that could cause interference to the Ag/AgCl ISEs response in concrete, stone, and seawater exposure [4, 24, 35, 44, 45]. It should be noted (Table 4) that iodide might be a potentially serious contaminant. However, iodide is not expected in relevant concentrations in the exposure regimes considered in this work. Moreover, it has been previously reported that iodide interference is actually smaller than generally assumed [41] and therefore, it is not addressed in this study.

With the exception of hydroxyl interference, the Ag/AgCl ISEs were first immersed in NaCl solutions without containing interfering species. Regarding the hydroxyl interference, experiments were always started with 0.1 mol L^{-1} sodium hydroxide solutions to simulate the alkalinity of the concrete pore solution. In this case, experiments were also carried out avoiding exposure to daylight as this may affect the results [46]. This would be an artifact because when the sensors are embedded in building materials, they are not exposed to daylight.

The concentration of the interfering species was increased stepwise as soon as the potential became stable over time (from a few minutes—for the addition of hydroxyl, sulfate, and fluoride—up to a few days—for the addition of bromide and sulfide). Ag/AgCl ISEs were immersed in the solutions containing increasing amounts of the possible interfering species for a total of 2 months.

The used solutions and the concentration ranges of interfering species are given in Table 3. The selected concentration ranges and their relation to practice for the case of stone and concrete are discussed in Sect. 4.2.

Once the experiments were finished, the Ag/AgCl ISEs that were immersed in the solutions containing bromide, fluoride, sulfate, and sulfide were immersed back into the initial NaCl solutions without interfering

Table 3 Solutions used for the study of the sensitivity to interfering species of the Ag/AgCl ISE

NaCl concentration (mol L^{-1})	Concentration range of interfering species (mol L^{-1})	Interfering species
0.05	0.1–1.7	OH^-
0.1	0.1–1.6	OH^-
0.2	0.1–1.5	OH^-
0.3	0.1–1.6	OH^-
0.5	0.1–1.6	OH^-
0.01	0–0.4	Br^-
0.1	0–0.3	Br^-
0.01	0–0.04	F^-
0.01	0–0.04	SO_4^{2-}
0.1	0–0.01	S^{2-}
1	0–0.008	S^{2-}

species. The potential was then measured after 1 month of immersion in the chloride solutions. The aim of this last experiment was to check whether prolonged exposure to the interfering species could compromise the functionality of Ag/AgCl ISEs once they are exposed again only to chlorides.

3.2.3 Long-term stability at high pH

The stability of the Ag/AgCl ISEs at high pH in the absence of chloride was investigated over a period of 60 days. Erlenmeyer flasks were filled to the very top with sodium hydroxide solutions and closed with a rubber plug through which the ISEs were inserted via drilled holes. The flasks were additionally sealed with silicon grease to avoid evaporation and/or carbonation of the solution.

The solutions used for the long-term stability were: 0.01 mol L^{-1} NaOH, 0.1 mol L^{-1} NaOH, and 1 mol L^{-1} NaOH. For comparison, 0.1 mol L^{-1} NaOH solution that contained always 0.1 mol L^{-1} NaCl was also used in this experiment.

After 60 days of immersion, sodium chloride was added to the chloride-free alkaline solutions up to a concentration of 0.1 mol L^{-1}.

4 Results and discussion

4.1 Calibration in solution

The calibration curve according to Eq. (6) is shown in Fig. 3.

The Ag/AgCl ISEs exhibit a Nernstian behavior with a slope of −59 mV/decade, in good agreement with the values reported in previous works [24, 27]. Furthermore, the standard deviation of the ten individual potential readings is always below 2 mV.

The ISEs exhibit Nernstian behavior in the interference-free solutions for the whole range of chloride concentrations tested (Fig. 3). It can be then concluded that the detection limit of the chloride ion in aqueous neutral solution is lower than 0.002 mol L^{-1}, in agreement with the results reported by Angst et al. [27].

4.2 Sensitivity to interfering species

4.2.1 Zones of interference

Figure 4 schematically illustrates the effect of the interfering species on the Ag/AgCl ISE response by dividing the diagram ISE potential versus activity of interfering species in three different regions.

In zone "a" (Fig. 4), the Ag/AgCl ISE behaves as an ideal chloride sensor. It exhibits a stable potential, determined by the chloride ion activity and independent on the interfering species [27, 29, 47]. It is in this range where the Ag/AgCl ISE is suitable for field measurements—namely, where it acts as "pure chloride sensor"—without interference. The effect on the chloride activity of the other ions present in the solution should however be taken into account.

When the concentration of interfering species increases (zone "b" in Fig. 4), the response of the ISE is altered and it shows a potential determined by the simultaneous action of primary (chloride) and

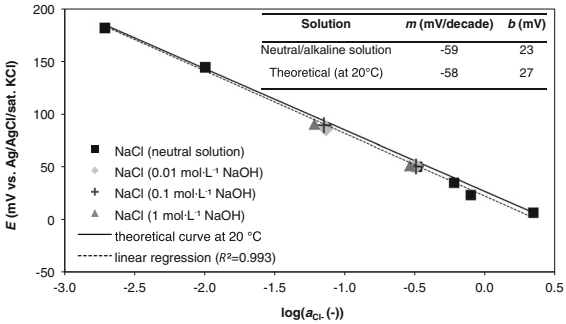

Fig. 3 Calibration curve for the Ag/AgCl ISE in neutral and alkaline solutions (mean values obtained from ten individual readings). The standard deviation is always less than 2 mV (smaller than the symbols). The parameters of the linear regression analysis are also given together with the theoretical values [42] (considering a constant room temperature of 20 °C)

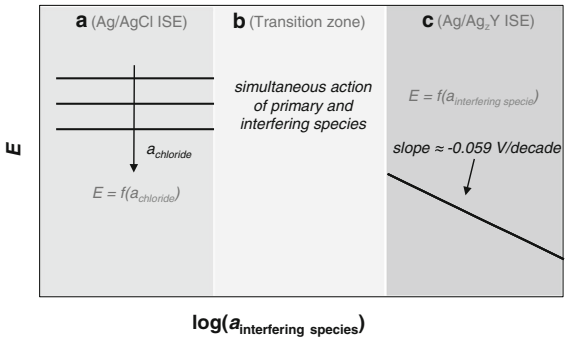

Fig. 4 Schematic Ag/AgCl ISE potential *E* as a function of the activity of the interfering species (at room temperature)

interfering species. This interference is reported to be due to the replacement of the chloride by the interfering species on the surface of the ISE [29, 47]. Different concentrations of primary and interfering species would lead to different stages in surface coverage of the precipitate formed between silver and interfering species [47]. No line was drawn for this region in Fig. 4 because the potential of the ISE is here depending on a number of factors, including time effects (see Appendix 1).

At sufficiently high concentrations of interfering species, the ISE surface becomes totally covered by the salt formed between silver and interfering species and then the ISE is only sensitive to this species [47, 48] (zone "c" in Fig. 4).

The response of the Ag/AgCl ISE will be in one of the three zones of Fig. 4 depending on how severe is the interference is and on the experimental conditions [29, 33, 47, 48]. In addition, it should also be noted that once the interfering species is removed from the solution, the Ag/AgCl ISE should ideally behave again as an ideal chloride sensor [35] (zone "a" in Fig. 4).

4.2.2 *Sensitivity to hydroxyl, bromide, fluoride, sulfate and sulfide*

In this work, the ideal ISE behavior shown in zone "a" in Fig. 4 is found for hydroxyl, fluoride, and sulfate for almost the whole range of tested concentrations.

Figure 5 gives the potential *E* of the Ag/AgCl ISEs immersed in alkaline solutions containing NaCl as a function of the hydroxyl concentration. The potential *E* of the Ag/AgCl ISEs was corrected for the liquid junction potential [Eq. (6)].

From Fig. 5, it can be seen that the Ag/AgCl ISEs do not significantly deviate from the potential registered in absence of hydroxyl (empty markers in Fig. 5). The maximum deviation with respect to this value is 8 mV and it is found for the ISEs immersed in the solution containing 0.05 mol L^{-1} NaCl. The difference between the largest and smallest observed potentials is 10 mV and it is also found for the ISEs immersed in the solution containing 0.05 mol L^{-1} NaCl.

Figure 6 gives the potential *E* of the Ag/AgCl ISEs immersed in 0.01 mol L^{-1} NaCl solution with increasing amount of fluoride and sulfate as a function of the concentration of these species. The potential

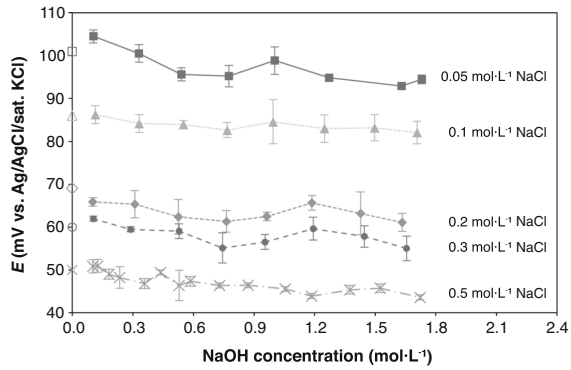

Fig. 5 Ag/AgCl ISE mean potential values (from five individual readings) as a function of the NaOH concentration. The *empty markers* (*left side* of the graph) indicate the potential at zero NaOH concentration obtained for the corresponding chloride concentration (calibration curve). The *error bars* indicate the standard deviation from the individual readings

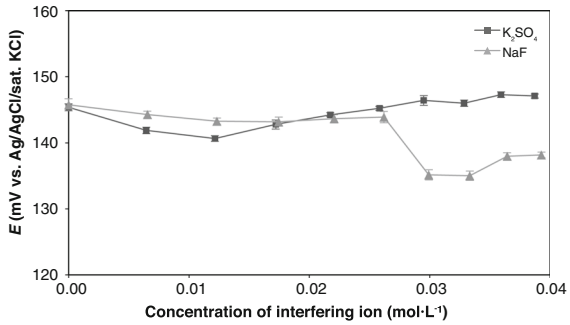

Fig. 6 Ag/AgCl ISE mean potential values (from ten individual readings) as a function of the NaF and K_2SO_4 concentrations in 0.01 mol L^{-1} NaCl solution. The potentials of both curves at zero NaF and K_2SO_4 concentration correspond to the mean value for the chloride concentration obtained from the calibration curve (Sect. 4.1). The *error bars* indicate the standard deviation from the individual readings

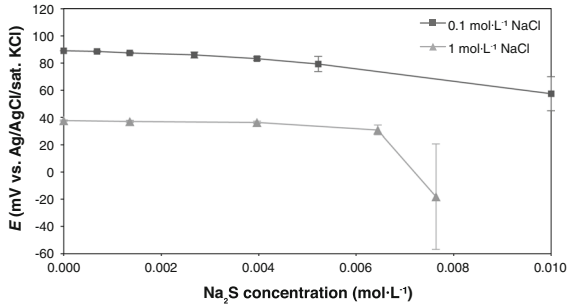

Fig. 7 Ag/AgCl ISE mean potential values (from ten individual readings) as a function of the Na_2S concentration. The potentials of both curves at zero Na_2S concentration correspond to the mean value for the chloride concentration obtained from the calibration curve (Sect. 4.1). *Error bars* indicate the standard deviation from the individual readings

E of the Ag/AgCl ISEs was also corrected for the liquid junction potential [Eq. (6)].

Regarding the fluoride interference, it is observed that up to a fluoride concentration of 0.02 mol L^{-1}, the ISE potential can be considered to be unaffected (Fig. 6). At fluoride concentrations higher than 0.025 mol L^{-1}, however, a small decrease in the potential is observed. For sulfate, the potential remains almost unaffected to—at least—a concentration of 0.04 mol L^{-1} (fourfold chloride concentration). Moreover, when returned back to the original NaCl solution (fluoride- and sulfate-free), the ISEs exhibit potentials equal to those initially registered in the absence of the interfering species within a few minutes.

For bromide and sulfide, the interference is more severe. Figure 7 shows the potential E of the Ag/AgCl ISEs immersed in 0.1 and 1 mol L^{-1} NaCl solutions with increasing amounts of sulfide. For the bromide interference, the potential E is plotted against the logarithm of the bromide concentration. This is shown in Fig. 8. The potential E of the Ag/AgCl ISEs shown in Figs. 7 and 8 was also corrected for the liquid junction potential [Eq. (6)].

In the presence of bromide and sulfide, the ISE exhibits the ideal behavior depicted in zone "a" in Fig. 4 only at low bromide and sulfide concentrations ($c_{KBr} < 0.01$ mol L^{-1} for the ISEs immersed in the solution containing 0.1 mol L^{-1} NaCl and $c_{Na_2S} < 0.006$ mol L^{-1} for both tested chloride solutions).

Relatively small amounts of sulfide and bromide cause high potential shifts. For sulfide concentrations above 0.006 mol L^{-1}, the registered ISE potential decreases more than 20 mV for the ISEs immersed in the 0.1 mol L^{-1} NaCl solution and more than 50 mV for the ISEs immersed in the 1 mol L^{-1} NaCl solution. The standard deviation also increases significantly at this sulfide concentration (Fig. 7), with values higher than 12 mV in both cases. For the bromide interference, strong potential shifts are observed at bromide concentrations higher than 0.01 and 0.02 mol L^{-1} for the ISEs immersed in the solutions containing 0.01 and 0.1 mol L^{-1} NaCl, respectively. The standard deviation is also high in this range, reaching values up to 25 mV. It should also be noted that the immersed tip of the ISEs turned green upon the addition of bromide. The same phenomenon was observed for the ISEs

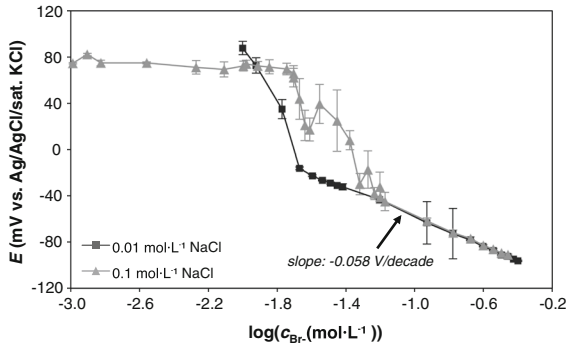

Fig. 8 Ag/AgCl ISE mean potential values (from ten individual readings) as a function of the KBr concentration. The potentials of both curves at zero KBr concentration correspond to the mean value for the chloride concentration obtained from the calibration curve (Sect. 4.1). *Error bars* indicate standard deviation between the individual readings

immersed in the solutions containing sulfide but, in this case, the tip of the ISEs turned black and it also decreased its thickness.

The significant potential decrease (at constant chloride concentration) and the high standard deviation for the sensors immersed in the same solution are an indication of the mentioned surface coverage process (Sect. 4.1) when both primary and interfering species act simultaneously (zone "b" in Fig. 4). The color change of the tip of the ISEs also evidences the surface coverage of the ISE with the salt formed with the interfering species.

For bromide concentrations higher than 0.05 mol L^{-1}, the potential E is governed by the bromide concentration for both tested chloride concentrations (Fig. 8). The slope in this part of the graph is −0.058 V/decade, thus exhibiting a Nernstian behavior. This corresponds to the zone "c" depicted in Fig. 4.

When returned back to the original NaCl solutions, the ISEs immersed in the solutions containing increasing amounts of bromide and sulfide did not regain the potential values that they initially exhibited for the given chloride solution. As pointed out in Sect. 4.1, once the interfering species is removed from the solution, the Ag/AgCl ISE should respond again to the chloride with Nernstian behavior (zone "a" depicted in Fig. 4). This was already reported by Atkins et al. [35] for the bromide interference. However, in this study, the ISEs were immersed in the solutions containing bromide for about 2 months, whereas Atkins et al. immersed them for only 15 min [35]. It is believed that this disagreement is due to the kinetics of the transformation of AgBr back into AgCl. In fact, Rhodes et al. [47] reported that the kinetics of the transformation of the AgBr back into AgCl is at least 200 times slower than the conversion of AgCl into AgBr. Thus, prolonged exposure to bromide and sulfide in the absence of significant amounts of chlorides may significantly impair the applicability of Ag/AgCl ISEs for field measurements.

4.3 Applicability of the Ag/AgCl ion-selective electrode in practical situations

As explained in Sect. 2.1, the interference from external species on the ISEs response is usually quantified with the selectivity coefficients. However, the kinetics of the reactions of the interfering species with the ISE surface is normally not considered. This issue is discussed in the Appendix 1 of this paper. Therefore, the use of selectivity coefficients appears not to be appropriate for evaluating interference at mid-long term exposure (see Appendix 1). In this work, the exposure time of the ISE to the possible interfering species was 2 months. From the obtained results, the applicability of the Ag/AgCl ISE for in situ measurements in concrete and stone is discussed in this section.

4.3.1 Concrete

Upon hydration of cement, high hydroxyl concentrations are typically present in the concrete pore solution. When it comes to chloride-induced corrosion of the reinforcement steel, a concentration ratio chloride to hydroxyl $c_{Cl^-}/c_{OH^-} = 0.6$ may as a fist-hand estimate be considered as threshold value for corrosion initiation [49]. As it is apparent from Fig. 5, no interference is found even for clearly lower ratios c_{Cl^-}/c_{OH^-}. Thus, the Ag/AgCl ISEs are feasible to monitor chloride ingress into concrete for the purpose of corrosion studies. It will allow detecting chloride concentrations much below levels considered critical for corrosion initiation even at high pH.

If concrete structures are exposed to seawater, bromide interference could be a potential issue. The bromide/chloride ratio in seawater is approximately 0.002 [50]. At a bromide/chloride ratio of 0.1 (for the ISEs immersed in 0.1 mol L^{-1} NaCl), no interference is here observed. Furthermore, from Fig. 8, it becomes apparent that the ISEs can tolerate slightly higher bromide concentrations when the chloride content is also higher. The chloride concentration in seawater is around 0.5 mol L^{-1} NaCl. Thus, no significant interference from bromide is expected in this case.

On the contrary, because of the severity of its interference, it is strongly suggested that the Ag/AgCl ISEs are not used when sulfide can be present in high amounts as, for example, in slag cement [44, 51, 52]. Moreover, slag cement is not a well-defined product, showing great variations of sulfide content in the different production plants and cement binders [44, 51–54]. Therefore, the influence on the sulfide concentration in the pore solution is difficult to predict and the question of whether the Ag/AgCl ISE can be used in the concretes containing mid-low amounts of blast furnace slag (for example, CEM III/A) seems

unclear and it has been already questioned by the authors [55].

The instability of the Ag/AgCl ISE at high pH with no or low presence of chlorides has also been questioned [24, 27, 45]. For this reason, the stability of the Ag/AgCl ISEs at high pH in absence of chloride was also investigated in this work. Figure 9 shows the potential E of as a function of time, before and after addition of chloride (at $t = 60$ days) for the chloride-free solutions. The potential E was corrected for the liquid junction potential [Eq. (6)].

In absence of chloride, the potential of the Ag/AgCl ISEs shows high scatter between the individual sensors (Fig. 9). In addition, the color of the solutions turned brown-black with time. This color change was more pronounced for the solutions that contained higher NaOH concentrations.

In alkaline environments in absence or low content of chlorides, the AgCl precipitate undergoes the following reaction [56]:

$$2AgCl_{(s)} + 2OH^- \rightleftarrows Ag_2O_{(s)} + H_2O + 2Cl^- \quad (7)$$

For the case of the Ag/AgCl ISEs immersed in chloride-free alkaline solutions (Fig. 9), the measured potential values were initially higher than 140 mV and they decreased to approximately 120 mV after 60 days of immersion. This suggests that the continuous formation of Ag_2O shifts the potential of the sensors to more negative values; potentials of $\sim$100 mV (vs. Ag/AgCl/sat. KCl) at room temperature and pH 14 are reported in the literature [27, 57]. The change of color observed can also be related to the transformation of AgCl into Ag_2O. This was already observed by Angst et al. [27]. The possible formation of Ag_2O [Eq. (7)] could explain the oscillations in the Ag/AgCl ISE potential shown in Fig. 5, especially at the lowest chloride concentrations.

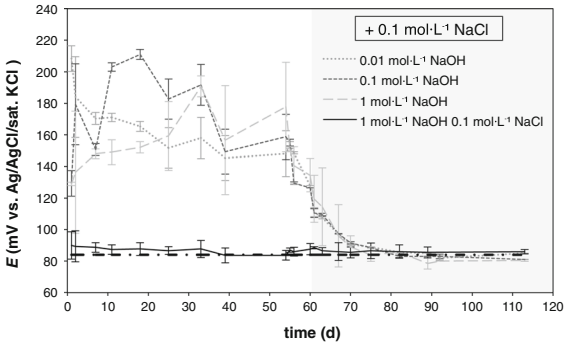

Fig. 9 Ag/AgCl ISE mean potential values (from ten individual readings) as a function of time. The *dash dot thick line* indicates the potential 0.1 mol L^{-1} NaCl solution (calibration curve). The *error bars* indicate the standard deviation from the individual readings. The beginning of the *grey shaded area* marks the addition of potential 0.1 mol L^{-1} NaCl

Upon addition of chloride, however, the ISEs exhibit the potential expected from the calibration curve within less than 8 days. The temporal scatter and instability are also considerably reduced. Thus, the possible formation of silver oxide is fully reversible, as it was already stated by Angst et al. [27] and Pargar et al. [57]. The adherence of the Ag_2O to the ISE surface (questioned by Angst et al. [27]) could however be an issue for the long-term stability because of the reversibility of the AgCl formation. This aspect should deserve further attention.

4.3.2 *Stone*

Silicates are the most common minerals in igneous, metamorphic and many sedimentary rocks [4]. However, stones may also contain other minerals in smaller quantities; the ones that can potentially interfere the response of the Ag/AgCl ISE are: galena (PbS), sphalerite (ZnS), fluorite (CaF_2), gypsum ($CaSO_4{\cdot}2H_2O$) and anhydrite ($CaSO_4$). On the basis of the values of solubility product at 25 °C (or equilibrium constant for the case of sulfide) reported in literature [38], the maximum amount of each species is here calculated and the possible interference discussed.

The maximum concentration of fluoride that can be found from the dissolution of pure fluorite is $c_{F^-} \approx 2 \times \left(\frac{K_{S\_CaF_2}}{4}\right)^{1/3} = 4 \times 10^{-4}$ mol L^{-1}. From Fig. 6, no interference is expected at such low concentrations. Following the same reasoning, the maximum amount of sulfate deriving from the dissolution of pure gypsum ($CaSO_4{\cdot}2H_2O$) and pure anhydrite ($CaSO_4$) is estimated to be 1.2×10^{-2} and 1.5×10^{-2} mol L^{-1}, respectively. From Fig. 6, no interference is found at those sulfate concentrations.

Regarding the presence of sulfide, it should be noted that S^{2-} is not present in significant concentrations due to the hydrolysis reaction of this ion with water [38, 58]. In this case, the solubility product of compounds containing sulfides Y_xS_z is replaced by the equilibrium constant K_{YS} of the following reaction:

$$Y_xS_z + zH^+ \rightleftarrows xY^{(2z/x)+} + zHS^- \quad (8)$$

Thus, the concentration c_{HS^-} of hydrogen sulfide ion derived from the dissolution of pure galena and pure sphalerite can be estimated as: $c_{HS^-} \approx \sqrt{K_{YS} \times c_{H^+}}$. In absence of carbonates, it can be assumed that the pH of the pore water in stone is neutral ($c_{H^+} \approx 10^{-7}$ mol L^{-1}). Therefore, the maximum concentrations of hydrogen sulfide ion are 8×10^{-12} and 1.4×10^{-8} mol L^{-1}, respectively, when pure galena (PbS) and pure sphalerite (ZnS) are present. From the obtained results (Fig. 7), no effect on the ISE response is expected at such low concentrations.

The data obtained in this study show that the above-listed minerals possibly present in stone should not interfere with the Ag/AgCl ISE response. The above-mentioned considerations are, however, valid for pure minerals and are given as general indications. A more complex environment (like the natural one) could substantially change these values due to the contemporary presence of other equilibria with the surrounding environment. For example, iodide may be expected in some organic-rich sedimentary rocks [59]. The possible interference in these cases should be then further tested and studied.

In addition, experience on the applicability of the Ag/AgCl in stone is very limited and more research in this field should be done.

4.3.3 Additional remarks on the applicability of the Ag/AgCl ISE for field measurements

Similar to the liquid junction potentials taken into account in this work, any concentration differences present between the ISE and the reference electrode will give rise to diffusion potentials that add arithmetically to the measured potential [60]. In porous systems such as concrete, stone, or soil, concentration gradients are likely to be present and maintained over long periods, due to the restricted mass transport in the tortuous pore systems. Thus, depending on the position of the reference electrode with respect to the ISE, these diffusion potentials may present a serious error source. This has been treated in detail elsewhere [60]. In general, to minimize these errors, the reference electrode should be placed as close to the ISE as possible.

5 Conclusions

The Ag/AgCl ISEs studied in this work responded to chloride, as expected from Nernst's law and previous studies.

The sensitivity of the Ag/AgCl ISE to other interfering species has been carefully studied in this work. While negligible interference was found for fluoride, sulfate, and hydroxyl, the interference is relatively severe for bromide and sulfide. Nevertheless, due the high chloride/bromide concentration ratio in seawater, the interference of bromide is considered negligible for applications in seawater exposure.

In completely chloride-free alkaline solutions, the ISEs were not stable over time, probably due to transformation reactions with the environment. Upon addition of chloride, however, the sensors responded again according to Nernst's law.

Based on the current experimental observations, it is concluded that the studied Ag/AgCl ISEs are feasible for practical monitoring of the chloride concentration in inorganic porous building materials, such as stone or concrete exposed to chloride-containing environments. A notable exception is concrete with high blast furnace slag content, where the presence of sulfides could strongly disturb the measurements.

Acknowledgments The financial support from the Swiss National Science Foundation (SNF) is kindly acknowledged. The authors would also like to thank Dr. Nicolas Roussel for his valuable comments to improve the manuscript.

Appendix 1

Limitations of the concept of selectivity coefficients (time effect)

The severity of the interference of external species with the ISE is commonly taken into account with the selectivity coefficients [see Eq. (3)] [30–33, 39]. The theoretical models for estimating selectivity coefficients are traditionally based on the assumption that thermodynamic equilibrium is established. In these models, the kinetics of the reactions is normally neglected.

Table 4 lists the selectivity coefficients $K^{pot}_{Cl^-,Y}$ of the Ag/AgCl ISE to other species reported in

Table 4 Values of selectivity coefficients $K^{pot}_{Cl^-,Y}$ for the Ag/AgCl ISE reported in literature and maximum allowable chloride to interfering species ratio not causing interference

Interfering species	Minimum allowable chloride to interfering species ratio [61]	Selectivity coefficient $K^{pot}_{Cl^-,Y}$	Exposure time to the solution with interfering species	Reference for the reported selectivity coefficient $K^{pot}_{Cl^-,Y}$
OH^-	1.25×10^{-2}	4×10^{-3}	>6 months	[27]
		2×10^{-3}–9.1×10^{-3}	<1 day	[62, 63]
		2.4×10^{-2}	Not specified	[29]
		9.33×10^{-3}	Theoretical model	Calculated from [39]
		$\approx 10^{-2}$	Theoretical model	[30]
		$\approx 10^{-2}$	Not specified	[36]
Br^-	3.33×10^{2}	2.1–3.3×10^{2}	<1 day	[64]
		1.1×10^{2}–3.5×10^{2}	<1 day	[62, 63]
		1.2	Not specified	[29]
		3.63×10^{2}	Theoretical model	Calculated from [39]
		1–3.5×10^{2}	Theoretical model	[30]
I^-	2×10^{6}	3–14	<1 day	[41]
		1.8×10^{2}–2.2×10^{6}	<1 day	[62, 63]
		86.5–1.8×10^{6}	<1 day	[64]
		86.5	Not specified	[29]
		2.9×10^{6}	Theoretical model	Calculated from [39]
		1–2.1×10^{6}	Theoretical model	[30]
S^{2-}	$>10^{6}$	2.04×10^{15}	–	Calculated from [39]
SO_4^{2-}		4.73×10^{-8}	–	Calculated from [39]

literature. Information about the theoretical or experimental calculation of the selectivity coefficients and the exposure time of the ISE in the solution containing interfering species (in the case of experimental calculation) is also given here. The values of the solubility products for the calculation of the theoretical selectivity coefficient according to Morf et al. [39] were obtained from the data reported by Haynes [38]. Table 4 also provides the minimum chloride to interfering species ratio tolerated without causing interferences reported by Kaland et al. [61].

In general, there is a large variability in the reported selectivity coefficients (Table 4). As a comparison, Eq. (3) is solved for the selectivity coefficient for the case of the bromide interference, yielding:

$$K^{pot}_{Cl^-,Br^-} = \frac{e^{\frac{\left(E^0_{Ag/AgCl} - E\right)F}{RT}}}{a_{Br^-}} - a_{Cl^-} \quad (9)$$

From the experiments performed in this study, all the parameters on the right side of Eq. (9) are known for each step of the increasing interference concentration. The values of chloride and bromide activity coefficients were obtained with the PHREEQC Interactive v. 3.1.4 software. Its computational routine is based on the specific ion interaction theory (SIT) and it models well chloride-based systems with ionic strength up to 1 mol L^{-1} [62]. Figure 10 shows the computed selectivity coefficient according to Eq. (9) as a function of the bromide concentration.

When the ISE acts as an ideal Ag/AgCl ISE (zone "a" in Figs. 4 and 10), the selectivity coefficient is relatively small, indicating that the contribution of the bromide is low and that the potential exhibited by the ISE is governed by the chloride content.

When the ISE acts only as AgBr ISE (zone "c" in Figs. 4 and 10), the values of the selectivity coefficient obtained for both tested chloride concentrations are similar and relatively constant. They are also in the same order of magnitude as most of the values reported in literature (Table 4). It should be noted, however, that, in this zone, the ISE is no longer a Ag/

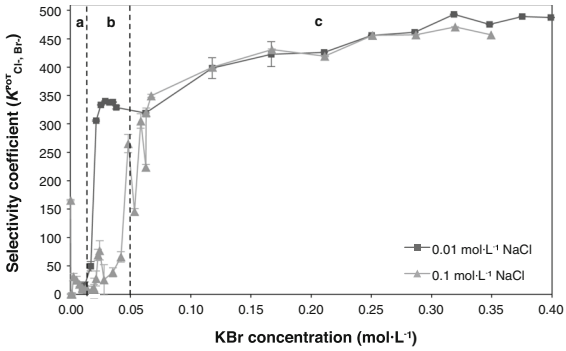

Fig. 10 Selectivity coefficient $K^{pot}_{Cl^-,Br^-}$ as a function of the bromide concentration calculated according to Eq. (9). The standard deviation (*error bars*) from the ten individual potential readings is always below 30 mV. The zones defined in Fig. 4 are here divided by *dashed lines*: *a* Ag/AgCl ISE, *b* transition zone, *c* Ag/AgBr ISE

AgCl ISE, but rather a Ag/AgBr ISE. Thus, the selectivity coefficient $K^{pot}_{Cl^-,Br^-}$—as it appears in Eq. (3)—does in principle not make sense.

When the chloride and bromide act simultaneously (zone "b" in Figs. 4 and 10), the selectivity coefficient suddenly rises, indicating the increasing interference of the bromide in this case. It is believed that, in this case, the ISE response is influenced by other parameters, such as the surface coverage, diffusion processes, membrane morphology, etc. [33, 41, 47, 48, 63–65]. This might also be the reason for the high variability of the selectivity coefficients found in literature.

In case of short-term exposures, as in the case of applications in analytical chemistry, the protocol described by the IUPAC [33] is recommended. However, it is believed that both thermodynamics and kinetics contribute to the selectivity of ion-selective electrodes. This has already been suggested by other authors [64, 66]. Therefore, it appears that the theoretical models for predicting the Ag/AgCl ISE response in presence of interfering ions are not suitable for mid to long-term exposure.

References

1. Elsener B, Bertolini L, Pedeferri P, Polder RP (2013) Corrosion of steel in concrete, 2nd edn. Wiley-VCH, Weinheim
2. Scherer GW (2004) Stress from crystallization of salt. Cem Concr Res 34:1613–1624. doi:10.1016/j.cemconres.2003.12.034
3. Angeli M, Benavente D, Bigas J-P, Menéndez B, Hébert R, David C (2007) Modification of the porous network by salt crystallization in experimentally weathered sedimentary stones. Mater Struct 41:1091–1108. doi:10.1617/s11527-007-9308-z
4. Siegesmund S, Snethlage R (2011) Stone in architecture: properties, durability, 4th edn. Springer, Berlin
5. Flatt RJ, Caruso F, Sanchez AM, Scherer GW (2014) Chemo-mechanics of salt damage in stone. Nat Commun 5:4823. doi:10.1038/ncomms5823
6. Ottosen LM, Rörig-Dalgaard I (2008) Desalination of a brick by application of an electric DC field. Mater Struct 42:961–971. doi:10.1617/s11527-008-9435-1
7. Bourgès A, Vergès-Belmin V (2010) Application of fresh mortar tests to poultices used for the desalination of historical masonry. Mater Struct 44:1233–1240. doi:10.1617/s11527-010-9695-4
8. Valenza JJ, Scherer GW (2006) Mechanism for salt scaling of a cementitious surface. Mater Struct 40:259–268. doi:10.1617/s11527-006-9104-1
9. Shi X, Fay L, Peterson MM, Yang Z (2009) Freeze–thaw damage and chemical change of a Portland cement concrete in the presence of diluted deicers. Mater Struct 43:933–946. doi:10.1617/s11527-009-9557-0
10. Angst U, Elsener B, Larsen CK, Vennesland Ø (2009) Critical chloride content in reinforced concrete—a review. Cem Concr Res 39:1122–1138. doi:10.1016/j.cemconres.2009.08.006
11. RILEM technical committee 235-CTC (2009) Corrosion initiating chloride threshold concentrations in concrete. http://www.rilem.org/gene/main.php?base=8750&gp_id=237
12. RILEM technical committee SCI (2014) Characteristics of the steel/concrete interface and their effect on initiation of chloride-induced reinforcement corrosion. http://www.rilem.org/gene/main.php?base=8750&gp_id=331
13. Geiker M, Nielsen EP, Herfort D (2006) Prediction of chloride ingress and binding in cement paste. Mater Struct 40:405–417. doi:10.1617/s11527-006-9148-2
14. Wall H, Nilsson L-O (2007) A study on sampling methods for chloride profiles: simulations using data from EPMA. Mater Struct 41:1275–1281. doi:10.1617/s11527-007-9325-y
15. Zheng JJ, Zhou XZ, Wu ZM (2009) A simple method for predicting the chloride diffusivity of cement paste. Mater Struct 43:99–106. doi:10.1617/s11527-009-9473-3
16. Juenger MCG, Winnefeld F, Provis JL, Ideker JH (2011) Advances in alternative cementitious binders. Cem Concr Res 41:1232–1243. doi:10.1016/j.cemconres.2010.11.012
17. Flatt RJ, Roussel N, Cheeseman CR (2012) Concrete: an eco material that needs to be improved. J Eur Ceram Soc 32:2787–2798. doi:10.1016/j.jeurceramsoc.2011.11.012
18. Chidiac SE, Panesar DK, Zibara H (2012) The effect of short duration NaCl exposure on the surface pore structure of concrete containing GGBFS. Mater Struct 45:1245–1258. doi:10.1617/s11527-012-9831-4
19. Kaminskas R, Barauskas I (2013) Influence of pozzolana on sulfate attack of cement stone affected by chloride ions. Mater Struct 47:1901–1910. doi:10.1617/s11527-013-0159-5

20. Vennesland Ø, Climent MA, Andrade C (2012) Recommendation of RILEM TC 178-TMC: testing and modelling chloride penetration in concrete. Mater Struct 46:337–344. doi:10.1617/s11527-012-9968-1
21. Cheewaket T, Jaturapitakkul C, Chalee W (2013) Concrete durability presented by acceptable chloride level and chloride diffusion coefficient in concrete: 10-year results in marine site. Mater Struct 47:1501–1511. doi:10.1617/s11527-013-0131-4
22. Atkins CP, Scantlebury JD, Nedwell PJ, Blatch SP (1996) Monitoring chloride concentrations in hardened cement pastes using ion selective electrodes. Cem Concr Res 26:319–324. doi:10.1016/0008-8846(95)00218-9
23. Climent-Llorca Miguel A, Viqueira-Pérez E, López-Atalaya MM (1996) Embeddable Ag/AgCl sensors for in situ monitoring chloride contents in concrete. Cem Concr Res 26:1157–1161. doi:10.1016/0008-8846(96)00104-4
24. Elsener B, Zimmermann L, Böhni H (2003) Non destructive determination of the free chloride content in cement based materials. Mater Corros 54:440–446. doi:10.1002/maco.200390095
25. Montemor MF, Alves JH, Simões AM, Fernandes JCS, Lourenço Z, Costa AJS, Appleton AJ, Ferreira MGS (2006) Multiprobe chloride sensor for in situ monitoring of reinforced concrete structures. Cem Concr Compos 28:233–236. doi:10.1016/j.cemconcomp.2006.01.005
26. Hugenschmidt J, Loser R (2007) Detection of chlorides and moisture in concrete structures with ground penetrating radar. Mater Struct 41:785–792. doi:10.1617/s11527-007-9282-5
27. Angst U, Elsener B, Larsen CK, Vennesland Ø (2010) Potentiometric determination of the chloride ion activity in cement based materials. J Appl Electrochem 40:561–573. doi:10.1007/s10800-009-0029-6
28. Garcia V, François R, Carcasses M, Gegout P (2013) Potential measurement to determine the chloride threshold concentration that initiates corrosion of reinforcing steel bar in slag concretes. Mater Struct 47:1483–1499. doi:10.1617/s11527-013-0130-5
29. Koryta J (1972) Theory and applications of ion-selective electrodes. Anal Chim Acta 61:329–411. doi:10.1016/S0003-2670(01)95071-8
30. Morf WE (1981) The principles of ion-selective electrodes and of membrane transport. Elsevier, New York
31. Koryta J, Stulik K (1983) Ion-selective electrodes, 2nd edn. Cambridge University Press, Cambridge
32. Janata J (1989) Principles of chemical sensors, 2nd edn. Plenum Press, New York
33. Lindner E, Umezawa Y (2008) Performance evaluation criteria for preparation and measurement of macro- and microfabricated ion-selective electrodes (IUPAC technical report). Pure Appl Chem. doi:10.1351/pac200880010085
34. Hidalgo A, Vera GD, Climent MA, Andrade C, Alonso C (2001) Measurements of chloride activity coefficients in real Portland cement paste pore solutions. J Am Ceram Soc 84:3008–3012. doi:10.1111/j.1151-2916.2001.tb01128.x
35. Atkins CP, Carter MA, Scantlebury JD (2001) Sources of error in using silver/silver chloride electrodes to monitor chloride activity in concrete. Cem Concr Res 31:1207–1211. doi:10.1016/S0008-8846(01)00544-0
36. de Vera G, Climent MA, Antón C, Hidalgo A, Andrade C (2010) Determination of the selectivity coefficient of a chloride ion selective electrode in alkaline media simulating the cement paste pore solution. J Electroanal Chem 639:43–49. doi:10.1016/j.jelechem.2009.11.010
37. Climent MA, Antón C, de Vera G, Hidalgo A, Andrade C (2011) The interference of OH^- ions in the potentiometric determination of free Cl^- in cement paste pore solution. In: Proceedings of the international RILEM conference on advances in construction materials through science and engineering, Hong Kong, China. RILEM Publications, Bagneux
38. Haynes WM (2013–2014) Handbook of chemistry & physics, 94th edn. CRC Press, Boca Raton
39. Morf WE, Kahr G, Simon W (1974) Theoretical treatment of the selectivity and detection limit of silver compound membrane electrodes. Anal Chem 46(11):1538–1543. doi:10.1021/ac60347a014
40. Bard AJ, Faulkner LR (2001) Electrochemical methods: fundamentals and applications, 2nd edn. Wiley, New York
41. Klasens HA, Goossen J (1977) The iodide interference with silver chloride electrodes. Anal Chim Acta 88(1):41–46
42. Shreir L (1994) Corrosion control. In: Shreir LL, Jarman RA, Burstein GT (eds) Corrosion, 3rd edn. Butterworth-Heinemann, Oxford
43. de Vera G, Hidalgo A, Climent MA, Andrade C, Alonso C (2000) Chloride-ion activities in simplified synthetic concrete pore solutions: the effect of the accompanying ions. J Am Ceram Soc 83(3):640–644. doi:10.1111/j.1151-2916.2000.tb01245.x
44. Chen W (2006) Hydration of slag cement—theory, modeling and application. PhD thesis, Enschede, University of Twente
45. Švegl F, Kalcher K, Kolar M (2006) In-situ detection of chlorides in capillary water of cementitious materials with potentiometric sensors. Eighth CANMET/ACI International Conference on Recent Advances in Concrete Technology. doi:10.14359/15913
46. Crowell RA, Lian R, Shkrob IA, Bartels DM, Chen X, Bradforth SE (2004) Ultrafast dynamics for electron photodetachment from aqueous hydroxide. J Chem Phys. doi:10.1063/1.1739213
47. Rhodes RK, Buck RP (1980) Competitive ion-exchange evaluation of the bromide interference on anodized silver/silver chloride electrodes. Anal Chim Acta 113:67–78. doi:10.1016/S0003-2670(01)85115-1
48. Hulanicki A, Lewenstam A (1977) Interpretation of selectivity coefficients of solid-state ion-selective electrodes by means of the diffusion-layer model. Talanta 24:171–175. doi:10.1016/0039-9140(77)80084-2
49. Hausmann DA (1967) Corrosion of steel in concrete. How does it occur? J Mater Prot 6:19–23
50. Dickson AG, Goyet C (1994) Handbook of methods for the analysis of the various parameters of the carbon dioxide system in sea water. US Department of Energy, Washington
51. Gollop RS, Taylor HFW (1996) Microstructural and microanalytical studies of sulfate attack: IV. Reactions of a slag cement paste with sodium and magnesium sulfate solutions. Cem Concr Res 26:1013–1028. doi:10.1016/0008-8846(96)00089-0

52. Taylor HFW (1997) Cement chemistry, 2nd edn. Thomas Telford, London
53. Lothenbach B, Le Saout G, Ben Haha M, Figi R, Wieland E (2012) Hydration of a low-alkali CEM III/B–SiO_2 cement (LAC). Cem Concr Res 42:410–423. doi:10.1016/j.cemconres.2011.11.008
54. Gruskovnjak A, Lothenbach B, Winnefeld F, Figi R, Ko SC, Adler M, Mäder U (2008) Hydration mechanisms of super sulphated slag cement. Cem Concr Res 38:983–992. doi:10.1016/j.cemconres.2008.03.004
55. Seguí-Femenias Y, Angst U, Elsener B (2015) Monitoring chloride concentrations in concrete by means of Ag/AgCl ion-selective electrodes. In: ICCRRR—international conference on concrete repair, rehabilitation and retrofitting (accepted), Leipzig
56. Biedermann G, Sillén LG (1960) Studies on the hydrolysis of metal ions. Part 30. A critical survey of the solubility equilibria of Ag_2O. Acta Chem Scand 14:717–725. doi:10.3891/acta.chem.scand.14-0717
57. Pargar F, Koleva DA, Koenders EAB, Breugel KV (2014) The importance of chloride sensors stability in monitoring ageing phenomena in concrete structures: Ag/AgCl electrodes performance in simulated pore-water environment. In: AMS 14: 1st ageing of materials & structures conference, Delft
58. Licht S (1988) Aqueous solubilities, solubility products and standard oxidation–reduction potentials of the metal sulfide. J Electrochem Soc 135:2971–2975. doi:10.1149/1.2095471
59. Nicholson K (1993) Geothermal fluids—chemistry and exploration techniques. Springer, Berlin
60. Angst U, Vennesland Ø, Myrdal R (2008) Diffusion potentials as source of error in electrochemical measurements in concrete. Mater Struct 42:365–375. doi:10.1617/s11527-008-9387-5
61. Kaland F, Hakli U, Ruoff P (1986) Use of an ion-selective electrode for determination of free chloride ions in water-based drilling fluids. SPE Drill Eng 1:365–368. doi:10.2118/15147-PA
62. Parkhurst DL, Appelo CAJ (2013) Description of input and examples for PHREEQC version 3—a computer program for speciation, batch-reaction, one-dimensional transport, and inverse geochemical calculations. U.S. Geological Survey Techniques and Methods, Denver
63. Moody GJ, Rigdon LP, Meisenheimerand RG, Frazer JW (1981) Selectivity parameters of homogeneous solid-state chloride ion-selective electrodes and the surface morphology of silver chloride-silver sulphide discs under simulated interference conditions. Analyst 106:547–556. doi:10.1039/AN9810600547
64. Hulanicki A, Lewenstam A (1982) Variability of selectivity coefficients of solid-state ion-selective electrodes. Talanta 29:671–674. doi:10.1016/0039-9140(82)80072-6
65. Radu A, Peper S, Bakker E, Diamond D (2007) Guidelines for improving the lower detection limit of ion-selective electrodes: a systematic approach. Electroanalysis 19:144–154. doi:10.1002/elan.200603741
66. Reinsfelder RE, Schultz FA (1973) Anion selectivity studies on liquid membrane electrodes. Anal Chim Acta 65:425–435. doi:10.1016/S0003-2670(01)82509-5